Ensemble Space-Time Correlation of Plasma Turbulence in the Solar Wind

W. H. Matthaeus

Bartol Research Institute, Department of Physics and Astronomy, University of Delaware, Newark, Delaware 19716, USA

J. M. Weygand

Institute for Geophysics and Planetary Physics, University of California, Los Angeles, California 90095, USA

S. Dasso

Instituto de Astronomía y Física del Espacio (IAFE) and Departamento de Ciencias de la Atmósfera y los Océanos and Departamento de Física, Facultad de Ciencias Exactas y Naturales, Universidad de Buenos Aires, 1428 Buenos Aires, Argentina

Single point measurement turbulence cannot distinguish variations in space and time. We employ an ensemble of one- and two-point measurements in the solar wind to estimate the space-time correlation function in the comoving plasma frame. The method is illustrated using near Earth spacecraft observations, employing ACE, Geotail, IMP-8, and Wind data sets. New results include an evaluation of both correlation time and correlation length from a single method, and a new assessment of the accuracy of the familiar frozen-in flow approximation. This novel view of the space-time structure of turbulence may prove essential in exploratory space missions such as Solar Probe Plus and Solar Orbiter for which the frozen-in flow hypothesis may not be a useful approximation.

Introduction.—The solar wind provides a natural laboratory for fundamental study of plasma turbulence in parameter ranges difficult to achieve in the laboratory (e.g., Ref. [1]) and often accessible only through remote sensing [2,3]. Fluctuations in space and time are characteristic of turbulence and each have significant influence in space and astrophysical contexts. The two-point correlation functions and associated spectra [4,5] are essential turbulence diagnostics in applications such as plasma heating [6], solar wind acceleration [7], the scattering and transport of energetic particles [8,9], magnetic field connectivity [10,11], and geospace prediction (space weather) [12]. Time correlation enters these applications as well, but in somewhat different ways [9,11], as is also well established in turbulence theory [13]. However, for most *in situ* interplanetary observations made by a single spacecraft there is an almost complete ambiguity between spatial structure and temporal structure. For fast flows, the Taylor frozen-in flow approximation [14] (or, *Taylor hypothesis*) provides an estimate of purely spatial statistics, with quantifiable limitations on accuracy [15–19]. The time correlation and the space correlation have not been previously treated on the same footing in interplanetary data sets, as far as we are aware. Here we employ a multispacecraft methodology to present a novel view of the space-time correlation of interplanetary turbulence. We show how numerous one- and two-spacecraft measurements may be combined, without use of the Taylor hypothesis, to determine correlation functions in which length and time separations are treated as independent. This method can provide a wealth of information about turbulence structure and dynamics, and may become a

valuable tool for interpreting present and future interplanetary data sets.

Background.—We consider space-time structure of fluctuations in interplanetary space. For simplicity we discuss only the magnetic field vector $\mathbf{B}(\mathbf{x}, t)$, a function of space $\mathbf{x}$ and time t coordinates. The dependent variables could also be velocity, density, temperature, or other quantities. The magnetic field $\mathbf{B}(\mathbf{x}, t) = \mathbf{B}_0 + \mathbf{b}$ is separated into ensemble mean $\langle \cdots \rangle$ and fluctuating parts; the mean is $\langle \mathbf{B} \rangle = \mathbf{B}_0$, the fluctuation (turbulence) is $\mathbf{b} = \mathbf{B} - \mathbf{B}_0$. The variance is $\sigma^2 = \langle |\mathbf{b}|^2 \rangle$. Usually the ensemble average is equivalent to a suitably chosen time averaging procedure. Of interest is the two-point, two-time correlation function

$$R(\mathbf{r}, \tau) = \langle \mathbf{b}(\mathbf{x}, t) \cdot \mathbf{b}(\mathbf{x} + \mathbf{r}, t + \tau) \rangle, \qquad (1)$$

which for stationarity and homogeneous turbulence is a function only of the spatial lag $\mathbf{r}$ and the time lag τ [20,21].

From $R(\mathbf{r}, \tau)$ in Eq. (1), one readily computes several quantities of interest in turbulence theory. For example, setting $\tau = 0$ one arrives at the two-point spatial correlation $R(\mathbf{r}) \equiv \langle \mathbf{b} \cdot \mathbf{b}' \rangle$, the prime here denoting a convenient abbreviation for the (spatially) lagged point. The correlation length (energy-containing scale) is defined as an integral, $\lambda_c \equiv \int_0^\infty R(r', 0, 0) dr' / \langle |\mathbf{b}|^2 \rangle$. The second order structure function $S(\mathbf{r}) = \langle |\mathbf{b} - \mathbf{b}'|^2 \rangle$ is found immediately from $R = \langle |\mathbf{b}|^2 \rangle - \frac{1}{2} S$. From the Fourier transform of $R(\mathbf{r})$ in $\mathbf{r}$, one obtains the magnetic energy spectrum, a quantity often discussed in the literature (e.g., Refs. [4,5,22]). Purely time domain statistics emerge upon setting $r = 0$ to obtain the Eulerian (one-point, two-time) correlation function

$R_E(\tau) = R(0,\tau) = \langle |\mathbf{b}(0,0) \cdot \mathbf{b}(0,\tau)|^2 \rangle$, which has deep ties to accelerations, intermittency, and sweeping effects in turbulence [23,24], and impacts scattering of energetic particles [9].

Measurement techniques.—The usual approach to compute two-point correlations (or spectra) in the solar wind employs single spacecraft measurements as a function of time, where the wind flows past the detector at super-Alfvénic and supermagnetosonic solar wind speed V_{sw}. In the (single-)spacecraft (*) frame one measures $R^*(0,\tau)$. The assumption that the structures measured are static during the time of passage of the detector leads to the relation $R^*(\hat{z}V_{\text{sw}}t, 0) \approx R^*(0, -t)$, where $\hat{z}$ is the direction of solar wind flow, usually very close to radial. This is the widely used Taylor hypothesis, which has also been used in some multispacecraft studies (e.g., Refs. [16–18]).

Here we do not invoke the Taylor hypothesis. Instead, a key step is to transform each measurement into the solar wind frame. A single spacecraft measurement transforms into the frame moving with the solar wind as

$$R^*(0,\tau) \to R(-\hat{z}V_{\text{sw}}\tau, \tau) \qquad (2)$$

where the $*$ indicates the spacecraft frame. We consider also two spacecraft (SC1 and SC2) measurements, where the (fixed) spatial separation of the pair is $\mathbf{r}_0$. Note that the extension of the Taylor hypothesis used by Osman and Horbury [15] is equivalent to $R^*(\mathbf{r}_0, \tau) \approx R(\mathbf{r}_0 - \hat{z}V_{\text{sw}}\tau, 0)$. Once again, such an approximation is not invoked here. Instead, one may also examine two-point measurement with SC1 data unlagged, and SC2 data transformed to the moving frame, and, therefore, without approximation accumulating a correlation that is lagged in both time and space. In that case, the transformation of a time lagged two-point correlation measurement to the solar wind frame becomes

$$R^*(\mathbf{r}_0, \tau) = \langle \mathbf{b}(0,0) \cdot \mathbf{b}(\mathbf{r}_0, \tau) \rangle \qquad (3)$$

$$\to R(\mathbf{r}_0 - \hat{z}V_{\text{sw}}\tau, \tau), \qquad (4)$$

where the magnetic field $\mathbf{b} = \mathbf{b}^*$ is invariant under the Galilean transformation.

Equation (4) provides the basis of the present technique for determining the space-time correlation: We compute correlation functions from many pairs of synchronized data sets, thus defining the ensemble of interest, and accumulate these in the solar wind frame, in the selected plane spanned by space lag and time lag; see Fig. 1.

Implementation and data sets.—We employ simultaneous epochs of synchronized vector magnetic field data recorded by the instruments on the ACE, Geotail, IMP-8, and Wind spacecraft [25–27]. A total number of more than 1000 pairs of such data sets are employed in the reported analysis. Previous publications describe the data sets, evaluation of stationarity, bad data removal, and the software framework, which has been well tested in related
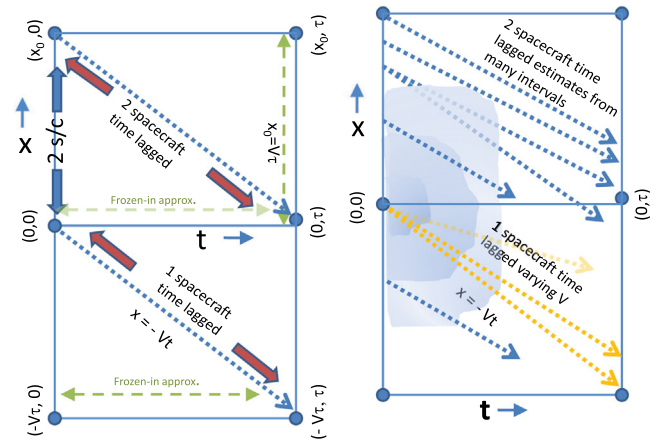

FIG. 1. (left) Space-time separation plane in the average solar wind plasma frame. Downward diagonal through the origin is the path observed by a single spacecraft (s/c). Vertical axis is the locus of pure spatial correlations. Taylor hypothesis approximates spatial correlation with single s/c correlation. The upper diagonal is the path observed by 2 s/c time-lagged correlations. (right) With many samples, it is feasible to obtain substantial information about the plasma frame space-time correlation. Here only one spatial coordinate is shown for simplicity.

studies [18,19,28]. The cleaned data are sorted into ranges of mean solar wind speed, an important organizing parameter for classifying types of solar wind streams.(see, e.g., Ref. [29]). Fast solar wind tends to be on average hotter, less dense, and more steady than slow solar wind. We will describe results obtained from the entire ensemble as well as subsets that include only fast solar wind intervals, and slow solar wind intervals, as defined below.

Results.—Each of the data sets were analyzed as follows. Each synchronized pair was subject to a time lagged correlation according to Eq. (4), in each case normalizing by the variance of the interval. A cross-correlation between the two spacecraft is computed, with intrinsic separation between the spacecraft $\mathbf{r}_0$, along with a time lag τ. Upon transformation into the frame moving with the mean plasma speed, each cross-correlation contributes a series of measurements along a diagonal of the type shown in the upper half of Fig. 1. Each time series is also individually analyzed as a time lagged, variance-normalized autocorrelation, which, in the mean solar wind frame, contributes the correlation in Eq. (4) with intrinsic separation vector $\mathbf{r}_0 = 0$, as illustrated in the lower half of Fig. 1.

To average the correlation estimates and cover the space-time plane with sufficient accuracy, a grid of space-time bins is established, and all estimates lying within a given bin are totaled, and then averaged when the selected ensemble is fully processed. A coarser grid gives higher statistical weight. The main results shown here are accumulated in bins of size 1.91×10^5 km in each resolved spatial direction, and 120 s in the time direction. After more than 1000 data set pairs are analyzed, the variation of solar wind speed and intrinsic spacecraft separation allows a
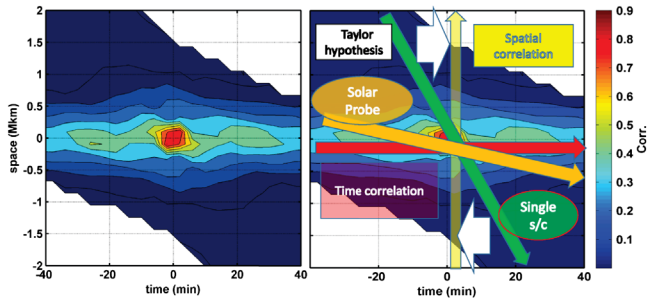
FIG. 2. (left) Space-time correlation of the full ensemble of solar wind magnetic field interval pairs described in the text, presented in the format $R(r, *, *, \tau)$, where the "$*$" indicate averaging over the transverse separations. (light) Same correlation, with annotations showing various sampling directions: spatial correlation, time correlation, fast single spacecraft trajectory, and slow spacecraft trajectory, such as Solar Probe. The content of the Taylor hypothesis is illustrated, as described in the text.

FIG. 3. Space-time correlation function $R(|\mathbf{r}|, \tau)$ as function of magnitude of separation $|\mathbf{r}|$ and τ, for samples of (left) slow wind and (right) fast wind. Note that the orientation of axes differs from Fig 2. The time axis is vertical, and to facilitate the fast or slow wind comparison, space separation increases towards the left (right) for the slow (fast) wind case.

large fraction of the correlation plane to be covered. The rendering by MATLAB routine CONTOURF provides a smooth interpolation in the space-time plane.

The accumulated averaged correlation data are displayed in Fig. 2 in the solar wind frame of reference. Plotted is the magnetic field autocorrelation $R(X, *, *, \tau)$, where the $*$ indicates an average over the associated Cartesian coordinate. The remaining spatial dependence X is the separation in the outward radial direction. As usual, τ is the time lag. A few features warrant immediate comment. The observed correlation function falls off almost monotonically from its central maximum. The decrease in the spatial direction occurs over a scale on the order of 10^6 km, consistent with the observed correlation scale near Earth orbit obtained by single spacecraft measurements employing the Taylor hypothesis [4] and with prior multiple spacecraft measurements [15,28]. In the time direction, the falloff occurs over a time scale of about 30–50 min. This too is consistent with previous multispacecraft estimates of the Eulerian decorrelation time [18,19] based on a different approach.

Figure 2 provides added annotation to aid interpretation. The vertical axis is the purely spatial correlation, related directly to the familiar spatial wave number spectra and structure functions that enter into the most familiar Kolmogorov ("5/3") theory of turbulence. This is usually not measured in the solar wind, but instead measurements are made along the main decreasing diagonal, in the spacecraft frame, as illustrated. This is intrinsically a mixture of space and time signals. As indicated in the figure, the Taylor hypothesis approximates as equal the values along the spacecraft frame diagonal and the vertical spatial correlation axis. The horizontal axis, as indicated in Fig. 2 corresponds to the purely time (or Eulerian) correlation, which to our knowledge has not been evaluated directly from data for any space plasma previously. Direct
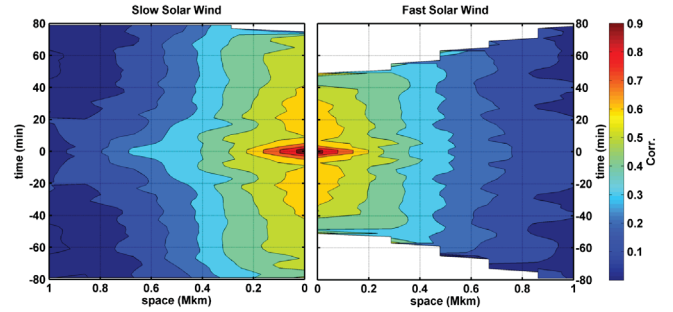
Eulerian measurement with a single spacecraft would require a detector moving outward at the solar wind speed.

To move towards more quantitative results, we accumulate separately data for fast ($V_{sw} > 550$ km/s) and slow (250 km/s $< V$sw < 450 km/s) solar wind mean velocity intervals. These ranges are chosen to approximate regimes associated with distinct behavior of temperature, density, and other properties as described for example by McComas et al. [29]. Here the correlation is expressed as a function of time lag τ and the magnitude of the vector separation $|\mathbf{r}|$. These two correlation functions are shown in Fig. 3. Note the change in format to facilitate this comparison is explained in the caption. The spatial extent of the fast and slow wind correlations is similar but it is immediately evident that the plasma frame slow wind correlation persists for larger time separations. This is consistent with a prior estimate in which only the time scale of decorrelation was estimated [19]. Table I shows quantitative comparisons of correlation scale λ_c, frozen-in flow correlation scale λ_c^*, and Eulerian correlation time T_c, obtained by separate analysis of fast and slow wind data. As anticipated, the correlation time and correlation length are both larger for the slow wind, which is consistent with the perspective that the slow wind is an older, more developed example of turbulence [30,31].

TABLE I. Correlation length $\lambda_c = \int_0^\infty R(r', 0, 0, 0) dr' / \langle |\mathbf{b}|^2 \rangle$, correlation length associated with single spacecraft frame using frozen-in flow $\lambda_c^* = \int_0^\infty R(V_{sw}\tau, 0, 0, \tau) dr' / \langle |\mathbf{b}|^2 \rangle$, and the correlation time $T_c = \int_0^\infty R(0, 0, 0, t') dt' / \langle |\mathbf{b}|^2 \rangle$, each for fast wind, slow wind, and total sample.

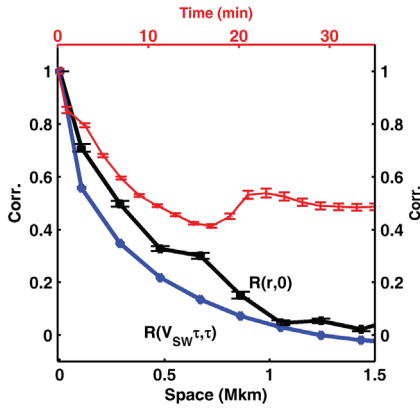|	Slow	Fast	All
λ_c (km)	441 000	395 800	434 900
λ_c^* (km)	223 100	259 400	234 400
T_c (s)	1914	1673	1720

FIG. 4. Correlation function $R(|\mathbf{r}|, \tau)$ sampled along three directions in space-time. (black, squares) Purely spatial correlation $R(r, 0)$ plotted vs r; (blue, diamonds) Typical observation made in a solar wind flow at speed V_{sw} by a single spacecraft, $R(V_{sw}\tau, \tau)$. These are approximated as equal in the Taylor hypothesis. Third curve (red, plus signs) is the purely temporal correlation $R(0, \tau)$ plotted vs τ on the upper axis. Error bars (standard error of the mean) are representative of counting statistics throughout the analysis.

Further examining these new results, one may readily verify that the correlation lengths reported in Table I are in the same range as many earlier single spacecraft results [30], and are about a factor of 2 smaller than earlier multispacecraft results [28]. This level of variability in different populations is not unexpected given that the distribution based on individual samples is broadly distributed (in fact, log-normal [31]). The Eulerian decorrelation time here is found to be longer in slow wind than in fast wind, as estimated earlier using a different (and more approximate) method [19]. The most significant difference with respect to that earlier case is that both fast and slow wind correlation times are a factor of 3 to 4 times smaller in the present case.

As a final diagnostic, one may compare the spatial decorrelation, the time correlation and the decorrelation seen by a typical spacecraft, by sampling the empirically determined correlation function along different directions in space-time. Figure 4 provides such a comparison, showing the $R(|\mathbf{r}|, \tau)$ correlation, sampled as $R(r, 0)$ vs r, $R(V_{sw}\tau, \tau)$ vs $r = V_{sw}\tau$, with V_{sw} the ensemble average solar wind speed, and $R(0, \tau)$ vs τ. The nearly flat region (and bump) beyond 0.9 Mm appears to be real and is suggestive of both a low frequency oscillation and a persistent long-time correlation. This will require further study. Quantitative comparison of the spatial correlation and the single spacecraft correlation provides a first illustration of the accuracy of the Taylor hypothesis. This comparison is made quantitative in Table II. One observes that the relative error in the frozen-in Taylor result is largest at large scales, and becomes smaller at smaller lags.

Discussion.—We have demonstrated a novel approach to assembling a space-time correlation from a collection of single spacecraft and two spacecraft solar wind

TABLE II. Comparison of correlation function $R(|\mathbf{r}|, 0)$ and its proxy from the Taylor hypothesis $R(V_{sw}\tau, \tau)$. Errors normalized to the sum of absolute values of the two estimates and are averaged over large, medium, and small ranges of scale.

Percent difference:	Slow	Fast	All
Large (1.0–1.3 Mkm)	100%	81.9%	100%
Medium (0.5–0.8 Mkm)	40.8%	16.9%	31.5%
Small (0.1–0.4 Mkm)	18.1%	10.1%	16.6%

observations, using no dynamical approximations and a minimal number of kinematic approximations (e.g., spacecraft motion is ignored within each interval). All correlation functions are fundamentally ensemble averaged quantities, and therefore will be sensitive to the properties defining the ensemble. Here we showed two versions: the first dependent on the radial coordinate and time, averaged over the transverse coordinates; the second depends on the magnitude of vector separation and time and was separated into fast wind and slow wind subensembles. Others are possible, for example, one might assume isotropy, or alternatively, axisymmetry, in which the spatial coordinates are resolved into components parallel to, and perpendicular to, the sample mean magnetic field directions. Further study in that direction will require substantial effort and is deferred to future publication.

We remark briefly on the relationship of this work to earlier studies in plasmas and fluids. Direct numerical simulation affords the opportunity to analyze the full space-time system in a straightforward way in fluids [32] as well as in magnetofluids [33] and plasmas [34,35]. We anticipate developing such results for comparison with solar wind correlations in the near future. The kinematic basis for assembling measurements in the space-time domain has been well understood in the fluid experiments [36–38] but not applied in space or plasma observations previously, to our knowledge.

Analytical study of the relationship between space correlations and time correlations has been an ongoing effort in turbulence theory, taking on two major approaches: First, for very small scales the correlations take on a simple interrelated elliptical form for homogeneous stationary turbulence [36]; this model has been revived at least several times [39–41]. This regime is not expected until small scales are probed, comparable to the dissipation scale [42]. A second major approach for analytical modeling is random sweeping, an idea originally developed by Heisenberg and later Kraichnan and collaborators [24,43]. Random sweeping provides a reasonable approximation in the inertial range of hydrodynamics [24,32] and magnetohydrodynamics [33,41], and is useful in applications such as cosmic ray scattering [9]; it may also be extended to include waves [44].

Because the space-time correlation is closely tied to turbulence theories [20] including closures (e.g., Ref. [13]), higher order statistics [23], and time variability [24], we

expect that the present work will open the door to a better integration of those theories into space and astrophysical plasma studies. The present results show how the space-time correlation in the solar wind may be determined experimentally. A next step is to employ theory and numerical simulations to further interpret and exploit these results. Refinements and extensions of these results are currently under way, and are expected to provide guidance for anticipating and explaining the observations to be made in the near future by exploratory missions such as Solar Probe Plus and Solar Orbiter.

[1] M. R. Brown and D. A. Schaffner, J. Plasma Phys. **81**, 345810302 (2015).

[2] J. Armstrong, J. Cordes, and B. Rickett, Nature (London) **291**, 561 (1981).

[3] M.-M. Mac Low and R. S. Klessen, Rev. Mod. Phys. **76**, 125 (2004).

[4] C.-Y. Tu and E. Marsch, Space Sci. Rev. **73**, 1 (1995).

[5] O. Alexandrova, C. H. K. Chen, L. Sorriso-Valvo, T. S. Horbury, and S. D. Bale, Space Sci. Rev. **178**, 101 (2013).

[6] B. J. Vasquez, C. W. Smith, K. Hamilton, B. T. MacBride, and R. J. Leamon, J. Geophys. Res. **112**, A07101 (2007).

[7] S. R. Cranmer, Space Sci. Rev. **172** 145 (2012).

[8] D. DeMarco, P. Blasi, and T. Stanev, J. Cosmol. Astropart. Phys. 06 (2007) 027.

[9] J. W. Bieber, W. H. Matthaeus, C. W. Smith, W. Wanner, M. Kallenrode, and G. Wibberenz, Astrophys. J. **420**, 294 (1994).

[10] J. Giacalone, J. R. Jokipii, and J. E. Mazur, Astrophys. J. Lett. **532**, L75 (2000).

[11] A. F. Rappazzo, W. H. Matthaeus, D. Ruffolo, S. Servidio, and M. Velli, Astrophys. J. **758**, L14 (2012).

[12] J. E. Borovsky, R. C. Elphic, H. O. Funsten, and M. F. Thomsen, J. Plasma Phys. **57**, 1 (1997).

[13] W. D. McComb, *The Physics of Fluid Turbulence* (Oxford University Press, New York, 1990).

[14] G. I. Taylor, Proc. R. Soc. A **164**, 476 (1938).

[15] K. T. Osman and T. S. Horbury, Astrophys. J. **654**, L103 (2007).

[16] J. D. Richardson and K. I. Paularena, J. Geophys. Res. **106**, 239 (2001).

[17] H. Matsui, C. J. Farrugia, and R. B. Torbert, J. Geophys. Res. **107**, SSH-7-1 (2002).

[18] W. H. Matthaeus, S. Dasso, J. M. Weygand, M. G. Kivelson, and K. T. Osman, Astrophys. J. Lett. **721**, L10 (2010).

[19] J. M. Weygand, W. H. Matthaeus, M. G. Kivelson, and S. Dasso, J. Geophys. Res. Space Phys. **118**, 3995 (2013).

[20] G. K. Batchelor, *The Theory of Homogeneous Turbulence* (Cambridge University Press, Cambridge, England, 1970).

[21] W. H. Matthaeus and M. L. Goldstein, J. Geophys. Res. **87**, 6011 (1982).

[22] F. Sahraoui, M. L. Goldstein, P. Robert, and Y. V. Khotyaintsev, Phys. Rev. Lett. **102**, 231102 (2009).

[23] M. Nelkin and M. Tabor, Phys. Fluids A **2**, 81 (1990).

[24] S. Y. Chen and R. H. Kraichnan, Phys. Fluids A **1**, 2019 (1989).

[25] C. W. Smith, J. L'Heureux, N. F. Ness, M. H. Acuña, L. F. Burlaga, and J. Scheifele, Space Sci. Rev. **86**, 613 (1998).

[26] S. Kokubun, T. Yamamoto, M. H. Acuña, K. Hayashi, K. Shiokawa, and H. Kawano, J. Geomagnet. Geoelect. **46**, 7 (1994).

[27] R. P. Lepping, M. H. Acuña, L. F. Burlaga, W. M. Farrell, J. A. Slavin, K. H. Schatten, F. Mariani, N. F. Ness, F. M. Neubauer, Y. C. Whang *et al.*, Space Sci. Rev. **71**, 207 (1995).

[28] W. H. Matthaeus, S. Dasso, J. M. Weygand, L. J. Milano, C. W. Smith, and M. G. Kivelson, Phys. Rev. Lett. **95**, 231101 (2005).

[29] D. J. McComas, L. Barraclough, H. O. Funsten, J. T. Gosling, E. Santiago-Muñoz, R. M. Skoug, B. E. Goldstein, M. Neugebauer, P. Riley, and A. Balogh, J. Geophys. Res. **105**, 10419 (2000).

[30] R. Bruno and V. Carbone, Living Rev. Solar Phys. **10**, 2 (2013).

[31] M. E. Ruiz, S. Dasso, W. H. Matthaeus, and J. M. Weygand, Sol. Phys. **289**, 3917 (2014).

[32] S. A. Orszag and G. S. Patterson, Phys. Rev. Lett. **28**, 76 (1972).

[33] S. Servidio, V. Carbone, P. Dmitruk, and W. H. Matthaeus, Europhys. Lett. **96**, 55003 (2011).

[34] T. N. Parashar, S. Servidio, M. A. Shay, B. Breech, and W. H. Matthaeus, Phys. Plasmas **18**, 092302 (2011).

[35] H. Comişel, D. Verscharen, Y. Narita, and U. Motschmann, Phys. Plasmas **20**, 090701 (2013).

[36] A. Favre, J. Gaviglio, and R. Dumas, Phys. Fluids **10**, S138 (1967).

[37] N. Mordant, Eur. Phys. J. B **76**, 537 (2010).

[38] M. Berhanu and E. Falcon, Phys. Rev. E **87**, 033003 (2013).

[39] G.-W. He and J.-B. Zhang, Phys. Rev. E **73**, 055303 (2006).

[40] X. Zhao and G.-W. He, Phys. Rev. E **79**, 046316 (2009).

[41] M. Wilczek and Y. Narita, Phys. Rev. E **86**, 066308 (2012).

[42] P. Chuychai, J. M. Weygand, W. H. Matthaeus, S. Dasso, C. W. Smith, and M. G. Kivelson, J. Geophys. Res. **119**, 4256 (2014).

[43] W. Heisenberg, Z. Phys. **124**, 628 (1948) [NACA Technical Memorandum 1431 (Washington, DC, Jan. 1958)].

[44] W. H. Matthaeus and J. W. Bieber, AIP Conf. Series **471**, 515 (1999).